Letter to the EditorA statistical study of the location and motion of the HF radar cusp

T. K. Yeoman, P. G. Hanlon, K. A. Mcwilliams

A statistical study of the location and motion of the HF radar cusp

T. K. Yeoman, P. G. Hanlon, and K. A. McWilliams

Department of Physics and Astronomy, University of Leicester, University Road, Leicester, LE1 7RH, UK

Abstract. The large-scale and continuous monitoring of the ionospheric cusp region offered by HF radars has been exploited in order to examine the statistical location and motion of the equatorward edge of the HF radar cusp as a function of the upstream IMF B_Z component. Although a considerable scatter is seen, both parameters have a clear influence from the north-south component of the IMF. Excellent agreement is achieved with previous observations from low altitude spacecraft data. The HF radar cusp region is seen to migrate equatorward at a rate of $0.02°\,\mathrm{min}^{-1}\,\mathrm{nT}^{-1}$ under IMF B_Z south conditions, but remains static for IMF B_Z north. The motion of the cusp implies an addition of magnetic flux of $\sim 2 \times 10^4\,\mathrm{Wb}\,\mathrm{s}^{-1}\,\mathrm{nT}^{-1}$ under IMF B_Z south conditions, equivalent to a reconnection voltage of $20\,\mathrm{kV}\,\mathrm{nT}^{-1}$, which is consistent with previous estimates from case studies on both the dayside and nightside regions.

Key words. Ionosphere (auroral ionosphere) – Magnetospheric physics (magnetosphere-ionosphere interaction; solar wind magnetosphere interactions)

1 Introduction

Reconnection on the dayside magnetopause is the dominant mechanism by which energy and momentum are transferred into the magnetosphere. Observations of both the magnetopause in situ and its ionospheric footprint have revealed these regions to be highly dynamic, and these dynamics represent an active area of magnetospheric research. Under southward interplanetary magnetic field (IMF) conditions, the transfer of magnetic flux from the IMF to the magnetosphere was initially interpreted as a steady-state process, although considerable evidence now exists for a time-dependent mechanism, where flux transfer occurs in the form of discrete episodes, termed Flux Transfer Events (FTEs) (see Smith et al., 1992; Milan et al., 2000; McWilliams et al.,

2001 and references therein). As new open flux is added to the dayside polar cap magnetosphere via such bursts of magnetic reconnection, the polar cap will adjust to a new equilibrium, with the polar cap boundary moving equatorward. HF coherent radars have provided a wealth of observations which have been associated with FTE activity and are an established tool for the study of such magnetopause processes via the monitoring of the large-scale electric fields which are imposed onto the dayside auroral zone ionosphere. The radars typically observe high velocity, anti-sunward transient flow in the cusp ionosphere. Such signatures were first assumed to be the response to transient magnetopause reconnection by Pinnock et al. (1993; 1995). HF radar data have since then demonstrated that the anti-sunward bursts of flow are associated with individual FTEs at the magnetopause (Neudegg et al., 1999). A more statistical examination was performed by Neudegg et al. (2000), who related the characteristic signatures of FTEs at the magnetopause, as observed by the Equator-S spacecraft, with the characteristic pulsed, anti-sunward flows observed in the HF radar data in the ionosphere, as detailed above, at the conjugate footprint of Equator-S. Neudegg et al. (2000) found a strong statistical association between the magnetopause and ionospheric phenomena. HF radar data are also characterised by an equatorward progression of the dayside auroral zone during a sequence of episodes of flux transfer, as the auroral zone tracks the expansion of the polar cap (e.g. McWilliams et al., 2001). Such data have also provided a wealth of information on the morphology, dynamics and scale size of the dayside reconnection process. Quasi-periodic sequences of such anti-sunward bursts of flow, termed pulsed ionospheric flows (PIFs), have been examined both statistically and individually, and the spatial extent of these events, their flow orientation, MLT occurrence and dependence on IMF have also been examined. The statistical location and extent of the HF radar cusp (identified via the characteristic pulsed antisunward flows) have been presented by Provan and Yeoman (1999), and the dependence on the IMF B_Y component was reported in Provan et al. (1999). Here, we exploit

Correspondence to: T. K. Yeoman
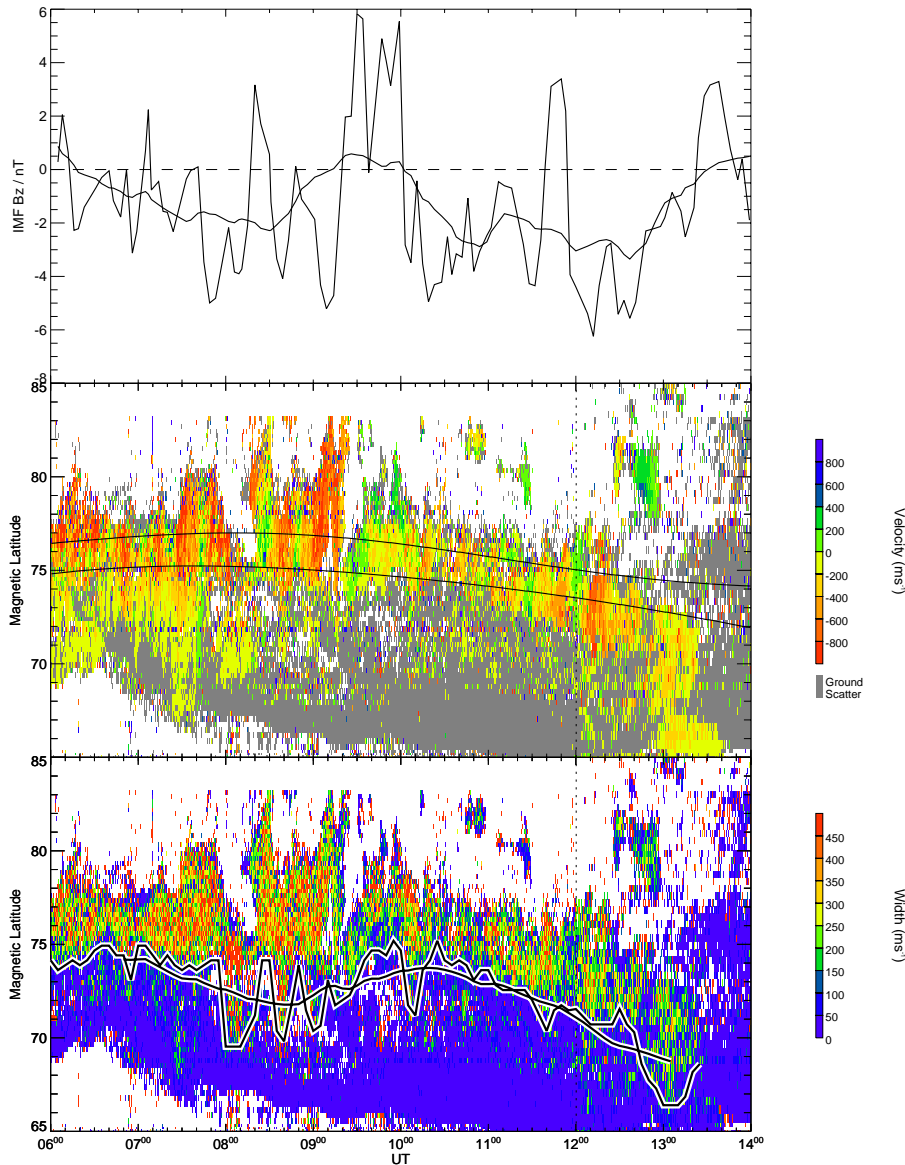(tim.yeoman@ion.le.ac.uk)

Fig. 1. An example of the identification of the HF radar cusp location and motion from 06:00–14:00 UT on 4 January 2000. The top panel presents the IMF B_Z component magnetic field data from ACE, timelagged by 68 min (see text for details). Both raw data at a time resolution of 5 min, and data smoothed over 50 min are shown. The middle panel presents line-of-sight velocity data from beam 9 of the SuperDARN Hankasalmi radar as a function of magnetic latitude and Universal Time. A statistical Feldstein oval is included for reference. The bottom panel presents beam 9 spectral width data in the same format. The equatorward edge of the region of high spectral width is marked with a line, at a time resolution of 5 min, and also smoothed over 50 min. Equatorward progression of the HF radar cusp is clearly related to intervals of southward (negative) IMF B_Z.

the large-scale and continuous monitoring of the ionospheric cusp region offered by the HF radar technique in order to explore both the statistical location and motion of the HF radar cusp as a function of the IMF B_Z component.

2 Observations

2.1 Instrumentation

The data analysed in this study are provided by the CUT-LASS Hankasalmi HF radar (Milan et al., 1997), which forms the easternmost element of the Northern Hemisphere SuperDARN array (Greenwald et al., 1995). The radar is frequency agile (8–20 MHz) and routinely measures the line-of-sight (l-o-s) Doppler velocity, spectral width and backscatter power from ionospheric plasma irregularities. The radar

forms 16 beams separated by 3.24°, each gated into 75 range gates. Here, we restrict ourselves to an analysis of the l-o-s velocity and spectral width data from the Hankasalmi beam 9, which is the meridionally directed beam. The prevailing IMF conditions are determined from the Advanced Composition Explorer (ACE) MFE instrument (Smith et al., 1998; Stone et al., 1998) and are reduced here to a time resolution of 5 min. The data are time-lagged in order to account for the propagation from the Sun-Earth L1 libration point to the dayside auroral ionosphere, using the technique outlined in Khan and Cowley (1999).

2.2 Data analysis

An example of the identification of the HF radar cusp is presented in Fig. 1, which covers the interval 06:00–14:00 UT (08:00–16:00 MLT) on 4 January 2000. The top panel
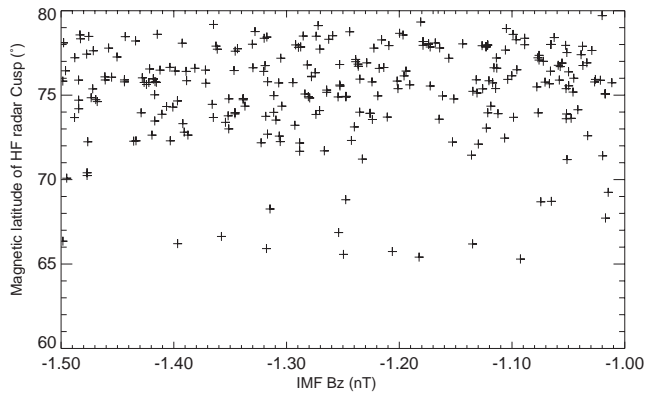
Fig. 2. Scatterplot of the locations of the HF radar cusp, such as those illustrated in Fig. 1, for prevailing IMF conditions with a southward (negative) IMF B_Z between -1.5 and -1.0 nT.

Fig. 3. The average location of the HF radar cusp as a function of the prevailing IMF B_Z component (solid line). The dashed lines represent ± 1 standard deviation of the distribution of latitude values. Only averages where more than 25 data points per bin were available are plotted.

presents the IMF B_Z component magnetic field data from ACE, time-lagged by 68 min, as described above. The data is presented at a time resolution of 5 min, and a time series boxcar averaged over 10 data points (50 min) is also presented. The middle panel illustrates the line-of-sight velocity data from beam 9 of the SuperDARN Hankasalmi radar as a function of magnetic latitude (Altitude Adjusted Corrected Geomagnetic coordinates are used here throughout; Baker and Wing, 1989) and Universal Time. The l-o-s velocities are colour-coded such that yellow and red represent negative Doppler shifts (poleward flow away from the radar). A statistical Feldstein auroral oval for $Q = 0$ (Feldstein, 1963; Holzworth and Meng, 1975) is indicated for reference. Pulsed, anti-sunward velocities, characteristic of HF radar cusp activity are clearly seen for almost the entire interval. The bottom panel presents the beam 9 spectral width data in the same format. Here the equatorward edge of the region of high spectral width is used as an indicator of the latitude of the equatorward boundary of the HF radar cusp. The high spectral width region corresponds to the cusp, as determined from low latitude particle signatures in a number of case studies (Baker et al., 1990; 1995), and this boundary (here taken to be $200 \, \mathrm{m \, s^{-1}}$) is marked with a line at a time resolution of 5 min. Again, a time-series boxcar averaged over 10 data points (50 min) is also plotted. The equatorward progression of the equatorward edge of the HF radar cusp (henceforth referred to here simply as the radar cusp) can be clearly related to intervals of southward (negative) IMF B_Z in the top panel, thus displacing the boundary equatorward of the statistical oval in the interval 07:30–09:30 UT, and after 10:30 UT. Here such locations and motions of the radar cusp are examined statistically for the months of December 1999 and January 2000, between 05:00–15:00 UT ($\sim$ 07:00–17:00 MLT, i.e. 10 h of local time spread symmetrically about noon). The MLT at which the radar cusp is observed is controlled by the IMF B_Y component, and such a range of local times will include the vast majority of radar cusp observations at Hankasalmi (Provan et al., 1999). The
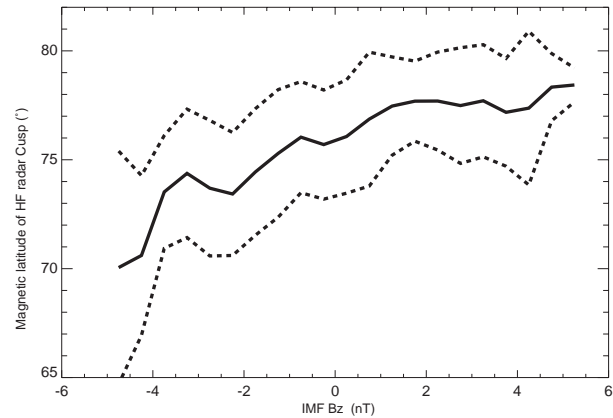
winter 1999/2000 interval is chosen to maximize the observation rate due to seasonal effects (Milan et al., 1997). This data set has provided some 300 h of simultaneous radar and spacecraft observations at 5 min resolution, with statistical analysis performed on the 50 min boxcar-averaged data sets, since short period fluctuations in the IMF and their effects in the dayside auroral zone are not the focus of the present study.

An example of the data from the statistical analysis is presented in Fig. 2, depicting a scatterplot of the locations of the radar cusp, such as those illustrated in Fig. 1, for prevailing IMF conditions with a southward (negative) IMF B_Z component between -1.5 and -1 nT. A considerable scatter is observed and will be discussed below. The mean location of the radar cusp as a function of IMF B_Z in 0.5 nT bins is illustrated in Fig. 3. A clear equatorward displacement of the average radar cusp location is apparent, with increasingly negative IMF B_Z, although the considerable scatter in the observations from this mean behaviour is evident from the lines marking ± 1 standard deviations from the mean in Fig. 3.

The large-scale and near-continuous monitoring of the location of the radar cusp offered by the HF radar technique allows for the use of the time series of the radar cusp location, such as those presented in Fig. 1, to calculate the evolution of the radar cusp location, as well as its average position. Figure 4 presents such an inferred radar cusp motion in degrees of latitude per minute, as a function of IMF B_Z. For positive B_Z, a near-static radar cusp location is evident. As B_Z turns negative, evidence of a clear and increasing equatorward motion is obtained, with a motion of $-0.08° \, \mathrm{min^{-1}}$ observed for IMF B_Z values of -4 nT.
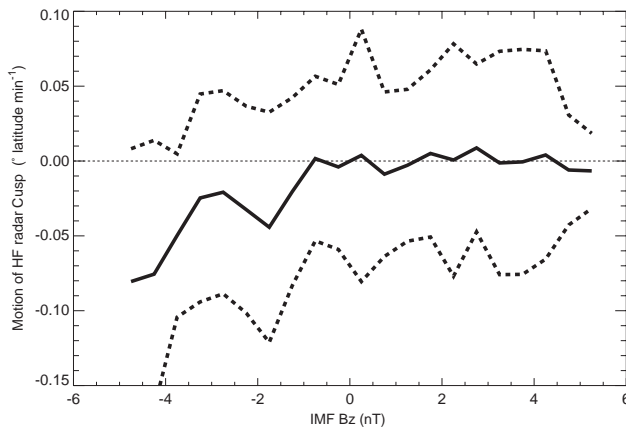
Fig. 4. The average motion of the HF radar cusp as a function of the prevailing IMF B_Z component (solid line). The dashed lines represent ± 1 standard deviation of the distribution of latitude variation values. Only averages where more than 25 data points per bin were available are plotted.

3 Discussion

The location and motion of the radar cusp is strongly influenced by the IMF B_Z component. However, it is clear from Figs. 2–4 that a considerable scatter characterises both parameters when organized solely by the IMF B_Z. In part, this is due to the history of the prevailing IMF conditions; the location of the cusp will respond to an integral of the IMF B_Z component for some prior period, and is also affected by substorm processes. The location of the ionospheric footprint of the cusp is also affected by the solar wind dynamic pressure (Zhou et al., 2000), and the IMF B_Y component (Newell et al., 1989; Provan et al., 1999), which have not been considered here. The MLT of the observation will also influence the observations, and this is illustrated in Fig. 1 via the statistical Feldstein oval. It is clear from Fig. 1 that the local time of observation will affect the deduced latitude of the HF radar cusp, with a change in the cusp latitude of $\sim 0.01°$ min^{-1} occurring due to local time effects. Since the local times chosen here for the statistical study are arranged symmetrically about noon, the effects of such variations will be apparent in the spread of values, rather than the averages obtained. The local time effects are also small, and thus equal in magnitude to the effect of an IMF B_Z south of just 1 nT. As a result, and due to the other effects which contribute to the spread of results detailed above, no explicit correction for MLT is applied to the results discussed below. In spite of the effects outlined above, the average latitude of the location of the radar cusp determined here (75°) corresponds very well to the equatorward boundary of the region of pulsed poleward flows (PPFs) observed by Provan et al. (1999) and Provan and Yeoman (1999). It is also in excellent agreement with the location of the equatorward boundary of the cusp as identified in the DMSP data by Newell and Meng (1988). All three of these studies also placed the boundary at 75°. Newell et al. (1989) explored the location of the equatorward edge of

the DMSP cusp as a function of IMF B_Z, which was placed at 73° for an IMF B_Z of -5 nT, increasing to 77° for a zero IMF B_Z, and then increasing more slowly to 78° as B_Z increased to $+5$ nT. Again, the HF radar data presented here is in close agreement. The variation with IMF is also similar to recent high altitude measurements (Zhou et al., 2000), although the actual latitudes deduced from the high altitude lie poleward of the low altitude satellite and the radar observations.

The motion of the radar cusp is examined in Fig. 4. For northward IMF, the location is seen to be static, as might be expected in the absence of subsolar dayside reconnection, which would add open flux. Lobe reconnection, unless occurring symmetrically in both hemispheres would leave the polar cap area unchanged. A closure of open flux due to symmetrical lobe reconnection for strongly northward IMF has been suggested by a number of authors (e.g. Dungey, 1963; Song and Russell, 1992). The present study suggests that such a process is rare and overall, not an important mechanism in the closure of polar cap magnetic flux, although it might be important in individual case studies. This finding is in accord with earlier suggestions by Fusilier et al. (1995). No evidence is seen for substorm processes in the current data set, which would destroy open flux, and this might be expected to reduce the polar cap area, thus displacing the radar cusp poleward. Presumably such substorm activity is averaged out in such a statistical study keyed to IMF B_Z. The motion of the radar cusp varies from $0.02°$ min^{-1} for IMF B_Z of -1 nT to $0.1°$ min^{-1} when B_Z decreases to -5 nT. Assuming a circular, incompressible polar cap, these values represent magnetic flux addition rates of 2×10^4 and 10^5 Wb s^{-1}, respectively, or equivalently dayside reconnection voltages of 20 and 100 kV. Such values are very similar to polar cap expansion rates inferred from the equatorward motion of HF radar data on the nightside during the substorm expansion phase (Lewis et al., 1998; Yeoman et al., 1999). The values of reconnection voltage also compare well with direct ionospheric measurements of the voltage associated with FTE activity of ~ 60 kV for IMF $B_Z = -5$ nT (McWilliams et al., 2001) and 160 kV for IMF $B_Z = -13$ nT (Milan et al., 2000). Taylor et al. (1996) have suggested values of flux addition of up to 5×10^5 Wb s^{-1} during magnetic storm intervals. Any quasi-steady-state reconnection activity in the distant magnetotail would act to close open magnetic flux, and thus reduce the area of the polar cap. Such activity is not accounted for in the above analysis of rates of additional open flux to the polar cap and reconnection voltages, and would need to be added to the figures presented above to obtain the true average dayside reconnection rates.

4 Summary

HF radar observations of the dayside auroral zone ionosphere have been used to identify the radar cusp via the characteristic signature of high spectral width coherent scatter echoes in the cusp region. This has allowed for a statistical exam-

ination of the location and motion of the equatorward edge of the HF radar cusp as a function of the upstream IMF B_Z component. Considerable scatter is observed, since the IMF B_Y component is not taken into account, which is known to affect the cusp location or the IMF history, which will also have a profound effect. In spite of this, the location and motion of the radar cusp are both clearly influenced by the north-south component of the IMF. Excellent agreement is achieved with previous observations from low altitude space-craft data. The radar cusp region is seen to migrate equatorward at a rate of $0.02°\,\mathrm{min}^{-1}\,\mathrm{nT}^{-1}$ under IMF B_Z south conditions, but remains static for IMF B_Z north. This motion of the radar cusp implies an addition of magnetic flux of $\sim 2 \times 10^4\,\mathrm{Wb\,s}^{-1}\,\mathrm{nT}^{-1}$ under IMF B_Z south conditions, equivalent to a reconnection voltage of $20\,\mathrm{kV\,nT}^{-1}$, which is consistent with previous estimates from case studies on both the dayside and nightside regions.

References

Baker, K. B. and Wing, S.: A new magnetic coordinate system for conjugate studies at high latitudes, J. Geophys. Res., 94, 9139, 1989.

Baker, K. B., Greenwald, R. A., Ruohoniemi, J. M., Dudeney, J. R., Pinnock, M., Newell, P. T., Greenspan, M. E., and Meng, C.-I.: Simultaneous HF radar and DMSP observations of the cusp, Geophys. Res. Lett., 17, 1869, 1990.

Baker, K. B., Dudeney, J. R., Greenwald, R. A., Pinnock, M., Newell, P. T., Rodger, A. S., Mattin, N., and Meng, C.-I.: HF radar signatures of the cusp and low-latitude boundary layer, J. Geophys. Res., 100, 7671, 1995.

Dungey, J. W.: The structure of the exosphere or adventures in velocityu space, in: Geophysics, The Earth's environment, (Eds) DeWitt, C., Hieblot, J., and LeBeau, A., 503–530, Gordon and Breach, New York, 1963.

Feldstein, Y. I.: On morphology of auroral and magnetic disturbances at high latitudes, Geomagn. Aeron., 3, 183, 1963.

Fuselier, S. A., Anderson, B. J., and Onsager, T.: Particle signatures of magnetic topology at the magnetopause: AMPTE/CCE observations, J. Geophys. Res., 100, 11, 805, 1995.

Greenwald, R. A., Baker, K. B., Dudeney, J. R., Pinnock, M., Jones, T. B., Thomas, E. C., Villain, J.-P., Cerisier, J.-C., Senior, C., Hanuise, C., Hunsucker, R. D., Sofko, G., Koehler, J., Nielsen, E., Pellinen, R., Walker, A. D. M., Sato, N., and Yamagishi, H.: Darn/Superdarn: A global view of the dynamics of high-latitude convection, Space Sc. Rev., 71, 761, 1995.

Holzworth, R. H. and Meng, C.-I.: Mathematical representation of the auroral oval, Geophys. Res. Lett., 2, 377, 1975.

Khan, H. and Cowley, S. W. H.: Observations of the response time of high-latitude ionospheric convection to variations in the interplanetary magnetic field using EISCAT and IMP-8 data, Ann. Geophysicae, 17, 1306, 1999.

Lewis, R. V., Freeman, M. P., and Reeves, G. D.: The relationship of HF radar backscatter to the accumulation of open magnetic flux prior to substorm onset, J. Geophys. Res., 103, 26, 613, 1998.

McWilliams, K. A., Yeoman, T. K., and Cowley, S. W. H.: Two-dimensional electric field measurements in the ionospheric footprint of a flux transfer event, Ann. Geophysicae, 18, 1584, 2001.

Milan, S. E., Yeoman, T. K., Lester, M., Thomas, E. C., and Jones, T. B.: Initial backscatter occurrence statistics for the CUTLASS HF radars, Ann. Geophysicae, 15, 703, 1997.

Milan, S. E., Lester, M., Cowley, S. W. H., and Brittnacher, M.: Convection and auroral response to a southward turning of the IMF: Polar UVI, CUTLASS and IMAGE signatures of transient magnetic flux transfer at the magnetopause, J. Geophys. Res., 105, 15, 741, 2000.

Neudegg, D. A., Yeoman, T. K., Cowley, S. W. H., Provan, G., Haerendel, G., Baumjohann, W., Auster, U., Fornacon, K.-H., Georgescu, E., and Owen, C. J.: A Flux transfer event observed at the magnetopause by the Equator-S spacecraft and in the ionosphere by the CUTLASS HF radar, Ann. Geophysicae, 17, 707, 1999.

Neudegg, D. A., Cowley, S. W. H., Milan, S. E., Yeoman, T. K., Lester, M., Provan, G., Haerendel, G., Baumjohann, W., Nikutowski, B., Büchner, J., Auster, U., Fornacon, K.-H., and Georgescu, E.: A survey of magnetopause FTEs and associated flow bursts in the polar ionosphere, Ann. Geophysicae, 18, 416, 2000.

Newell, P. T. and Meng, C.-I.: The cusp and the cleft/boundary layer: low-altitude identification and statistical local time variation, J. Geophys. Res., 93, 14, 549, 1988.

Newell, P. T., Meng, C.-I., and Sibeck, D. G.: Some low-altitude cusp dependencies of the interplanetary magnetic field, J. Geophys. Res., 94, 8921, 1989.

Pinnock, M., Rodger, A. S., Dudeney, J. R., Baker, K. B., Newell, P. T., Greenwald, R. A., and Greenspan, M. E.: Observations of an enhanced convection channel in the cusp ionosphere, J. Geophys. Res., 98, 3767, 1993.

Pinnock, M., Rodger, A. S., Dudeney, J. R., Rich, F., and Baker, K. B.: High spatial and temporal resolution observations ofthe ionospheric cusp, Ann. Geophysicae, 13, 919, 1995.

Provan, G. and Yeoman, T. K.: Statistical observations of the MLT, latitude and size of pulsed ionospheric flows with the CUTLASS Finland radar. Ann. Geophysicae, 17, 855, 1999.

Provan, G., Yeoman, T. K., and Cowley, S. W. H.: The influence of the IMF B_Y component on the location of pulsed flows in the dayside ionosphere observed by an HF radar, Geophys. Res. Lett., 26, 521, 1999.

Smith, M. F., Lockwood, M., and Cowley, S. W. H.: The statistical cusp: A flux transfer event model, Planet. Space Sci., 40, 1251, 1992.

Smith, C. W., Acuña, M. H., Burlaga, L. F., L'Heureux, J., Ness, N. F., and Scheifele, J.: The ACE Magnetic Fields Experiment, Space Sci. Rev., 86, 611, 1998.

Song, P. and Russell, C. T.: Model of the formation of the low-latitude boundary layer for strongly northward interplanetary magnetic field, J. Geophys. Res., 97, 1411, 1992.

Stone, E. C., Frandsen, A. M., Mewaldt, R. A., Christian, E. R., Marglies, D., Ormes, J. F., and Snow, F.: The Advanced Composition Explorer, Space Sci. Rev, 86, 1, 1998.

Taylor, J. R., Yeoman, T. K., Lester, M., Emery, B. A., and Knipp, D. J.: Variations in the polar cap area during intervals of substorm activity on 20–21 March 1990 decuced from AMIE convections patterns, Ann. Geophysicae, 14, 879, 1996.

Yeoman, T. K., Lewis, R. V., Milan, S. E., and Watanabe, M.: An interhemispheric study of the ground magnetic and ionospheric electric fields during the substorm growth phase and expansion phase onset, J. Geophys. Res., 104, 14, 867, 1999.

Zhou, X. W., Russell, C. T., Le, G., Fuselier, S. A., and Scudder, J. D.: Solar wind control of the polar cusp at high altitude, J. Geophys. Res., 105, 245, 2000.